Contemporary Mathematics
http://ojs.wiserpub.com/index.php/CM/

Research Article

A Vertical Surface Flow Analysis of MHD Nanofluids Influenced by Radiation, Viscous Dissipation, and Joule Heating with Soret and Dufour Effects

S. Jayanthi, H. Niranjan*

Department of Mathematics, School of Advanced Sciences, Vellore Institute of Technology, Vellore 632014, India
E-mail: hari.niranjan10@gmail.com

Received: 18 January 2024; **Revised:** 20 February 2024; **Accepted:** 29 February 2024

Abstract: The purpose of this study is to investigate the effects of radiation and activation energy on mass transfer nanofluids flowing across an expanding sheet in a vertical direction, as well as joule heating, viscous dissipation, Soret and Dufour, and magnetohydrodynamic (MHD) flow. The boundary layer (BL) equations for nonlinear momentum, energy, solute, and nanoparticle volume fraction are reduced by using similarity transformations. After that, the shooting technique and bvp4c are used to numerically solve the boundary layer equations. Schmidt and Eckert's numbers, along with Soret effects on velocity, temperature, and the volume percentage of nanoparticles, cause an increase in skin friction. Fluid temperature rises significantly with Eckert number. As the Dufour and Schmidt numbers rise, so does the local Nusselt number. A greater thermophoresis parameter, enhanced skin friction, and an increased Schmidt number.

***Keywords*:** joule heating, viscous dissipation, Soret/Dufour effects, MHD, nanofluid

MSC: 65L10, 80A20

1. Introduction

Acting as a viscous dissipation energy source, it impacts heat distribution and heat transmission rates. The effectiveness of viscous dissipation depends on whether the plate is frozen or heated. The joule heating acts as a heat source, similar to viscous fluid flow dissipation. Very few applications in actual life involve the employment of heat in ejection, paper manufacture, and electronic chip cooling, which relies on cooling rates and stretching procedures to achieve desired qualities. Most researchers are focused on this type of area because there are lots of applications in this field. So I have taken the literature from Lakshmi Devi [1] and Khan [2] to motivate this research.

Thermal radiation is a medium that converts thermal energy into electromagnetic energy. Thermal radiation is distinct from heat conduction and thermal convection; it is present in any region of a magnetic wave where the temperature is higher than zero. Kirchhoff's law can describe the properties of thermal radiation. These characteristics include emissive power, surface area, temperature, and absorption coefficient. Crucial to space technology is understanding the effect of radiation on heat transfer and flow in high-temperature processes. Furnaces, jet engines, power plants, gas turbines,

DOI: https://doi.org/10.37256/cm.5220244318

nuclear reactors, glassmaking, spaceships, satellites, and rockets are just a few of the numerous applications of the thermal radiation effect, which transmits heat.

Kumar et al. [3] explored the impacts of radiation on the three-dimensional flow and heat transmission of a Jeffrey nanofluid, including the role of viscous dissipation and Joule heating. Thermodynamic first law and its consequences on joule heating, radiation, and dissipation in relation to energy attribution are explored by Khan et al. [4]. Shahzad et al. [5] investigated the effect of alumina nanoparticles, titanium oxide, and silver on the flow with viscous dissipation and Joule heating over a Jeffrey fluid. The Soret and Dufour effects of an exponentially expanding surface on the unsteady transport of energy nanofluid in magnetohydrodynamics (MHD) were discussed by Siddique et al. [6] and Pal et al. [7]. To explore the process of radiative transfer, researchers employ variables such as thermal conductivity and mixed convection effects. The implications of micropolar nanofluids with non-isothermal flow by using the Cattaneo-Christov model on an MHD generator across a non-linearly increasing sheet are discussed by Ali et al. [8]. There is a chance that the study's physical and geometric components might provide results that are useful for thermally efficient devices. Muhammad et al. [9] investigated viscous flow in a three-dimensional stretch under the influence of (PHF) and (PCF) fluxes. Dusty Casson fluid flow, including the impacts of Marangoni convection, viscous dissipation, and Joule heating, was discussed by Mahanthesh et al. [10].

The Dufour effect is the cumulative result of irreversible processes that result in an energy flux when a mass concentration gradient is present. The Soret effect is the opposite phenomenon. The important effects are geosciences and chemical engineering. Niranjan et al. [11] and Lakshmi Devi et al. [1] discussed numerically the effects of Rd and chemical reactions on MHD flow in a porous medium incorporating diffusion-thermo and thermo-diffusion effects. Convective heat exchange simulation of viscous fluid flow with heat radiation and slip effects is examined numerically by Ullah et al. [12] along a vertically symmetric warmed plate submerged in a porous medium. Sreedevi et al. [13] scrutinize the effects of radiation on mixed-hollow density (MHD) flow and mass and heat transfer through a stretched, permeable sheet. Soret-Dufour effects in numerous slips and thermal aspects of Joule heating. It was Ali et al. [14] and Ahammad et al. [15] who examined the nanofluid Casson-Williamson relevance of investigating the mass transport and heat properties of Casson fluids along particular concentrations and thermal impacts. In their discussion of mixed convection mass transfer over an inclined plate, Mondal et al. [16] and Shankar et al. [17] addressed the influence of a non-uniform MHD, heat source/sink, thermophoresis, and chemical reaction.

Naseem et al. [18] investigated a hydromagnetized BL flow with varying viscous dissipation and temperature effects. Mat et al. [19] explored a horizontal channel with thermal radiation, Soret, and Dufour effects on the flow of the Jeffrey fluid. Chemical reactions on the flow of MHD nanofluid with viscous dissipation across a vertical plate in a rotating system were analyzed by Padmaja et al. [20]. Ghachem et al. [21] and Kumar et al. [22] scrutinized the viscoelastic fluid's Soret and Dufour features as caused by viscous dissipation in a moving cylinder. Ashraf et al. [23] concentrated on the periodic behavior of viscous dissipation impacts along the conducting electrical cone submerged in the porous medium and the convective heat transfer properties of fluid flow. Mahanthesh et al. [24] studied the unstable 3-D magnetohydrodynamic flow caused by a stretching surface. Muduly et al. [25] and Huang et al. [26] analyzed the impacts of viscous dissipation and joule heating on Casson nanofluid movement across a sheet of stretched material with a chemical reaction. In addition, it examines the heat and mass that are transported as fluid flows convectively through a porous medium. The stretching sheet movement of a nanofluid with electrical conductivity is numerically analyzed by Seid et al. [27] and Devi et al. [28].

Activation energy is the tiny quantity of energy added to the system to initiate a chemical reaction. The breaking of bonds in chemical reactions relies on two primary energies: kinetic and potential. Due to an improper impact, of kinetic energy there are instances where the molecular reaction is not completed. The oil storage industry and Hydrodynamics, geothermal power are three areas where activation energy is particularly useful. The magic of activation energy has been the subject of multiple investigations.

Kumar et al. [29] discussed the impacts of mhd flow and Cr behavior on Carreau fluid and found that a stronger concentration field is produced by a higher activation energy parameter. The activation energy, mass and heat transfer characteristics, and behavior of a viscous fluid undergoing radiation in a rotating frame were discussed by Sivasankaran et al. [30] and Yesodha et al. [31]. Additionally, the inquiry delves into the heat transfer related to fluid movement in

a rotating frame. Yesodha et al. [32] determined how a chemical reaction's activation energy affects a fluid's ability to transport heat and mass as measured by the (Hg) and (Rd).

A mathematical model is employed for the theoretical analysis of tangent hyperbolic nanoparticles with electrical maximum heat dissipation (MHD), activation energy, and Wu's slip properties, as discussed in Khan et al. [2] and Ibrahim et al. [33]. The local Nusselt number is unaffected by the convective parameter and power-law index. Over a non-conducting horizontal cylinder, Ullah et al. [34] discussed how the impact of the variable slip velocity is influenced by the surface temperature, free stream oscillation velocity, and mixed convection flow of an electrically conducting fluid. Gaffar et al. [35] studied the heat transmission of an indestructible tangent hyperbolic fluid from the sphere and the nonlinear stable flow of the boundary layer. Makinde et al. [36] and Rahman et al. [37] examined how the boundary layer's flow, heat transmission, and the proportion of nanoparticles over the surface of stretching in a nanofluid are affected by a convective boundary condition. Swain et al. [38] explored how viscous dissipation and joule heating affect MHD flow and heat transmission across a stretching sheet in porous media.

The primary aim of this work is to investigate the results of joule heating and viscous dissipation on the MHD mixed convection flow of a nanofluid across a vertically extended sheet when radiation, activation energy, Soret, and Dufour effects are present. The similarity transformations are applied to translate the governing Eqn's into ordinary ODEs. After that, the resultant equations can be derived to apply MATLAB bvp4c. Solute concentration, nanoparticle volume fraction, temperature, velocity, skin friction, heat, and mass transfer coefficients are studied and illustrated as a function of different flow parameters.

The novelty of this study is that the impact of viscous and joule heating on MHD flow and heat transfer is of interest because of the flow's significant role in a variety of devices that are subject to significant variations in gravitational force, as well as its application in heat exchanger designs, wire and glass fiber drawings, and various electric heating gadgets, such as irons, ovens, room warmers, geysers, and more, rely on the heating impact of current to function. Home wiring and electrical devices can be protected by using electric fuses, which work by utilizing the heating effect.

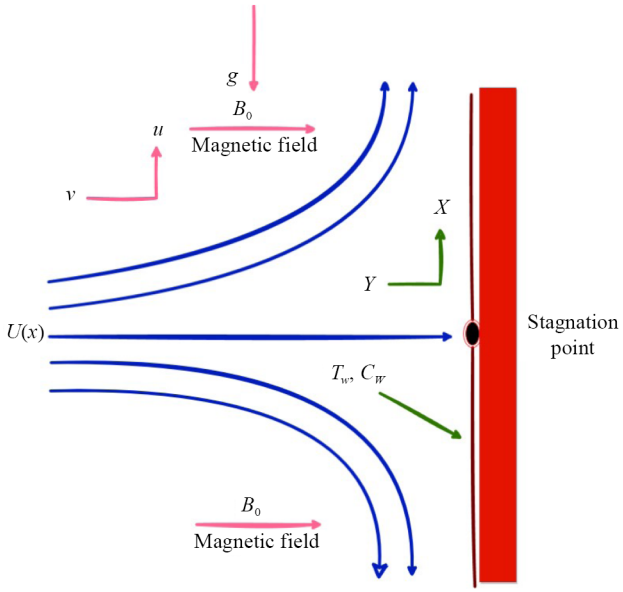

Figure 1. Schematic diagram of the problem

2. Mathematical analysis

Using radiation effects, imagine a steady, laminar, incompressible, multi-homogeneous nf flow over a stretched surface in a vertical orientation.The activation energy, viscous dissipation and Joule heating are all taken into account in

this particular case.Here we can see the coordinate system and physical model in Figure 1. Here the system of points (x, y), 'x' are selected to the surface, 'y' are selected normal to the surface. The x-axis measures the velocity component u, whereas the y-axis measures v.

Ordinarily, Magnetic field exerts its influence on the flow field intensity B_0. Pretend that vertical sheet surface is extended by the velocity $u_w = cx$, where $c > 0$ denotes the stretching rate constant. T_w, S_w and C_w are the wall-based measurements of temperature, solute concentration and nanoparticle volume fraction, while T_∞, S_∞, C_∞ represent the values distant from the wall. Solute, mass, nanoparticle, momentum and thermal energy governing equations can be expressed as

$$\frac{\partial v}{\partial y} + \frac{\partial u}{\partial x} = 0 \tag{1}$$

$$v^{\frac{\partial u}{\partial y}} + u\frac{\partial u}{\partial x} = v_f \frac{\partial^2 u}{\partial y^2} + \frac{1}{\rho_f}\left[(1-c_\infty)\rho_{f\infty}\beta(T-T_\infty) - (\rho_p - \rho_{f\infty})(c-c_\infty)\right] g - \frac{\sigma\beta_0^2}{\rho_f}u \tag{2}$$

$$v\frac{\partial T}{\partial y} + u\frac{\partial T}{\partial x} = -\frac{\alpha}{k}\frac{\partial q_r}{\partial y} + \alpha\frac{\partial^2 T}{\partial y^2} + \beta k_r^2 \left(\frac{T}{T_\infty}\right)^n exp\left[\frac{-E_a}{kT}\right](S - S_\infty)$$

$$+ \tau\left[D_B\frac{\partial T}{\partial y}\frac{\partial C}{\partial y} + \frac{D_T}{T_\infty}\left(\frac{\partial T}{\partial y}\right)^2\right] + \frac{D_m K_T}{c_s c_p}\left(\frac{\partial^2 S}{\partial y^2}\right) + \frac{\sigma B^2}{\rho cp}u^2 + \frac{\mu}{\rho c_P}\left(\frac{\partial u}{\partial y}\right)^2 \tag{3}$$

$$v\frac{\partial S}{\partial y} + u\frac{\partial S}{\partial x} = D\frac{\partial^2 S}{\partial y^2} + \frac{D_m K_T}{T_\infty}\left(\frac{\partial^2 T}{\partial y^2}\right) - K_r^2(S^- S_\infty^)\left(\frac{T}{T_\infty}\right)^n exp\left(\frac{-E_a}{KT}\right) \tag{4}$$

$$v\frac{\partial C}{\partial y} + u\frac{\partial C}{\partial x} = \frac{D_T}{T_\infty}\frac{\partial^2 T}{\partial y^2} + D_B\frac{\partial^2 C}{\partial y^2} \tag{5}$$

where $\alpha = \dfrac{k}{(\rho c)_f}$ and $\tau = \dfrac{(\rho c)_p}{(\rho c)_p}$.

Under the restrictions on the boundaries are,

$$D_\infty\frac{\partial c}{\partial y} + \frac{D_T}{T_\infty}\frac{\partial T}{\partial y} = 0,\ v = 0,\ S = S_w\ -k\frac{\partial T}{\partial y} = h_f(T_f - T),\ u = u_w(x) = cx,\ \text{at}\ y = 0 \tag{6}$$

$$C \to C_\infty,\ S \to S_\infty,\ T \to T_\infty u \to 0\ \text{as}\ y \to \infty \tag{7}$$

Arrhenius equation is $K_r^2\left(\dfrac{T}{T_\infty}\right)^n exp\left[\dfrac{-E_a}{KT}\right](S - S_\infty)$.

q_r is radiative heat flux given by

$$q_r = -\frac{4\sigma^*}{3K'}\frac{\partial T^4}{\partial y} \tag{8}$$

From Eqn (3), the radiative heat flux (q_r) term is simplified by using Rosseland Approximation. Ignoring higher-order terms. Using Taylor's series expansion T^4 about T_∞ and i.e., $T^4 = T_\infty + 4T_\infty^3(T - T_\infty) + ...$, then: $T^4 \approx 4T_\infty^3 T - 3T_\infty^4$, we get,

$$q_r = -\frac{16\sigma^* T_\infty^3}{3K'}\frac{\partial T}{\partial y} \tag{9}$$

The similarity variable η and non-dimensional functions $f(\eta)$, $\theta(\eta)$, $\chi(\eta)$, $\phi(\eta)$ defined as

$$\begin{gathered}\theta(\eta) = \frac{T - T_\infty}{T_w - T_\infty},\ \phi(\eta) = \frac{C - C_\infty}{C_w - C_\infty},\ v = -\sqrt{c}vf(\eta),\ \chi(\eta) = \frac{S - S_\infty}{S_w - S_\infty},\\ \psi(x,\ y) = \sqrt{c}vxf(\eta),\ \eta = \sqrt{\frac{c}{v}}y,\end{gathered} \tag{10}$$

$\psi(x,\ y)$ = stream function is defined as

$$v = -\frac{\partial \psi}{\partial x} \text{ and } u = \frac{\partial \psi}{\partial y} \tag{11}$$

An ODE system can be derived from the governing Eqn's. (1)-(5) by using Eqn's. (9)-(11).

$$f''' + \lambda(\theta - Nr\phi) - f'^2 + ff'' - Mf' = 0 \tag{12}$$

$$\begin{aligned}&PrNb\theta'\phi' + Pr\sigma Nc\chi[1 + \theta\delta]^n exp\left(\frac{-E}{1 + \theta\delta}\right)\\ &+ Prf\theta' + EcMPrf'^2 + NtPr\theta'^2 + PrEcf''^2 + \theta''\left(1 + \frac{4}{3}Rd\right) + D_f\chi'' = 0\end{aligned} \tag{13}$$

$$\chi'' + Scf\chi' + ScSr\theta'' - Sc\sigma\chi(1 + \theta\delta)^n exp\left(\frac{-E}{1 + \theta\delta}\right) = 0 \tag{14}$$

$$\phi'' + \left(\frac{Nt}{Nb}\right)\theta'' + Scf\phi' = 0 \tag{15}$$

The boundary conditions, become

$$\chi(0) = 1,\ f'(0) = 1,\ \phi'(0) = -\left(\frac{Nt}{Nb}\right) * \theta'(0),\ f(0) = 0,\ \theta'(0) = -Bi[1 - \theta(0)],\ \text{at } \eta \longrightarrow 0 \tag{16}$$

$$\chi(\infty)=0,\ \ \phi(\infty)=0,\ \ f'(\infty)=0,\ \ \theta(\infty)=0,\ \text{as}\ \ \eta\longrightarrow\infty \tag{17}$$

Now we introduced the nondimensional quantities are,

$$\begin{gathered}
Pr\ (\text{Prandtl number})=\frac{v_f}{\alpha_f},\ \ \lambda\ (\text{Mixed convection parameter})=\frac{g\beta(1-c_\infty)(T_w-T_\infty)}{C^2x}=\frac{Gr_x}{Re_x^2},\\
Sc\ (\text{Schmidt number})=\frac{v_f}{D_B},\ \ Gr_x\ (\text{Local Grashof number})=\frac{g\beta(1-c_\infty)(T_w-T_\infty)x^3}{v^2},\\
Ec\ (\text{Eckert number})=\frac{U_w^2}{c_p(T_w-T_\infty)},\ \ M\ (\text{Magnetic parameter})=\frac{\sigma_e B_0^2}{\rho_f c},\\
Nr\ (\text{Buoyancy ratio parameter})=\frac{\left(\rho_p-\rho_{f\infty}\right)(C_w-C_\infty)}{\rho_{f\infty}\beta(1-C_\infty)(T_w-T_\infty)},\ \ E\ (\text{Activation Energy})=-\frac{E_a}{KT_\infty},\\
Nb\ (\text{Brownion diffusion parameter})=\frac{\tau D_B C_\infty}{v_f},\ \ Bi\ (\text{Biot number})=\frac{h_f}{k}\sqrt{\frac{v}{c}},\\
Nt\ (\text{Thermoporesis parameter})=\frac{\tau D_T(T_w-T_\infty)}{T_\infty v_f},\ \ Sr\ (\text{Soret number})=\frac{D_m K_T\,(T_w-T_\infty)}{T_\infty v\,(S_w-S_\infty)},\\
\sigma\ (\text{Dimensionless reaction rate})=\frac{K_r^2}{c},\ \ D_f\ (\text{Dufor number})=\frac{D_m K_T\,(S_w-S_\infty)}{c_s c_p\alpha\,(T_w-T_\infty)},\\
Rd\ (\text{Thermal Radiation})=\frac{4\sigma^* T_3^\infty}{kK'},\ \ \delta\ (\text{Temperature difference parameter})=\frac{T_w-T_\infty}{T_\infty},\\
Nc\ (\text{Regular buoyancy parameter})=\frac{\beta(S-S_\infty)}{T_w-T_\infty},\ \ Re_x\ (\text{Local Reynolds number})=\frac{xU_w(x)}{v},\\
\nu\ (\text{Viscosity of the fluid})=\frac{\mu}{\rho},\ \ K\ (\text{Boltzmann constant})=8.61\times10^{-5}\ eV/K
\end{gathered} \tag{18}$$

3. Important quantities

$$\text{local Nusselt number } Nu_x = \frac{xq_w}{k(T-T_\infty)}, \quad \text{local Sherwood number } Sh_x = \frac{xq_s}{D_S(S-S_\infty)},$$

$$\text{local nanoparticle Sherwood number } Nn_x = \frac{xq_n}{D_B(c-c_\infty)}, \tag{19}$$

$$\text{local skin friction } C_f = \frac{\tau_w}{\rho U_w^2}.$$

where

$$\text{shear stress } (\tau_w),\ \tau_w = \mu\left[\frac{\partial u}{\partial y}\right]_{y=0}, \quad \text{surface heat flux } (q_w),\ q_w = -K\left[\frac{\partial T}{\partial y}\right]_{y=0},$$

$$\text{surface nanoparticle mass flux } (q_n),\ q_n = -D_B\left[\frac{\partial C}{\partial y}\right]_{y=0},$$

$$\text{surface mass flux } (q_s),\ q_s = -D_s\left[\frac{\partial S}{\partial y}\right]_{y=0}.$$

The physical quantities that we received in their dimensionless form are as follows.

$$C_f(Re_x)^{\frac{1}{2}} = f''(0), \quad \frac{Nu_x}{(Re_x)^{\frac{1}{2}}} = -\theta'(0), \quad \frac{Sh_x}{(Re_x)^{\frac{1}{2}}} = -\chi'(0), \quad \frac{Nn_x}{(Re_x)^{\frac{1}{2}}} = -\phi'(0). \tag{20}$$

4. Numerical method

The shooting technique is used to numerically solve the nonlinear ODE's (12)-(15) that are subject to bc's (16)-(17). To achieve this goal, allow

$$f = y_1,\ \phi' = y_9,\ f'' = y_3,\ \theta' = y_5,\ \chi = y_6,\ \chi' = y_7,\ \phi = y_8,\ \theta = y_4,\ \chi = y_6,\ f' = y_2 \tag{21}$$

The following first-order ordinary differential equations are obtained by converting equations (12)-(15):

$$f''' = y_2^2 - y_1y_3 + My_2 - \lambda(y_4 - Nry_8) \tag{22}$$

$$\theta'' = \left[\frac{1}{\left(1+\frac{4}{3}Rd+D_fScSr\right)}\right]\left(D_fScy_1y_7+D_fSc\sigma y_6[1+y_4\delta]^n exp\left(\frac{-E}{1+y_4\delta}\right)\right.$$

$$\left.\left\{-Pry_1y_5-NbPry_5y_9-NtPry_5^2-Pr\sigma y_6Nc(1+y_4\delta)^n exp\left(\frac{-E}{1+y_4\delta}\right)-EcMPry_2^2-PrEcy_3^2\right\}\right) \tag{23}$$

$$\chi'' = -Scy_1y_7+Sc\sigma y_6(1+y_4\delta)^n exp\left(\frac{-E}{1+y_4\delta}\right)$$

$$-ScSr\left(\left[\frac{1}{\left(1+\frac{4}{3}Rd+D_fScSr\right)}\right]\left(D_fScy_1y_7+D_fSc\sigma y_6[1+y_4\delta]^n exp\left(\frac{-E}{1+y_4\delta}\right)\right)\right.$$

$$\left.\left\{-Pry_1y_5-NbPry_5y_9-NtPry_5^2-Pr\sigma y_6Nc(1+y_4\delta)^n exp\left(\frac{-E}{1+y_4\delta}\right)-EcMPry_2^2-PrEcy_3^2\right\}\right)\right) \tag{24}$$

$$\phi'' = Scy_1y_9-\left(\frac{Nt}{Nb}\right)\left(\left[\frac{1}{\left(1+\frac{4}{3}Rd+D_fScSr\right)}\right]\left(D_fScy_1y_7+D_fSc\sigma y_6[1+y_4\delta]^n exp\left(\frac{-E}{1+y_4\delta}\right)\right)\right.$$

$$\left.\left(-Pry_1y_5-NbPry_5y_9-NtPry_5^2-Pr\sigma y_6Nc(1+y_4\delta)^n exp\left(\frac{-E}{1+y_4\delta}\right)-EcMPry_2^2-PrEcy_3^2\right)\right)\right) \tag{25}$$

with respect to the bc's (boundary conditions)

$$y_5(0) = -Bi[1-y_4(0)]\ y_1(0)=0,\ y_9(0) = -\left(\frac{Nt}{Nb}\right)y_5(0),\ y_2(0)=1,\ y_6(0)=1\ \text{ at }\ \eta\longrightarrow 0, \tag{26}$$

$$y_6(\infty)=0,\ y_8(\infty)=0,\ y_2(\infty)=0,\ y_4(\infty)=0,\ \text{ as }\ \eta\longrightarrow\infty \tag{27}$$

5. Results and discussion

Within the scope of the current research, the effects of D_f, Sr, and Rd and the passing of a vertical surface with E in the MHD nanofluid flow (activation energy) are all investigated. Applying BC's. (16)-(17) enables MATLAB bvp4c to find solutions to the governing equations. (12)-(15). The impression of a number of dimensionless parameters on $f'(\eta)$, $\theta(\eta)$, $\chi(\eta)$, $\phi(\eta)$ as well as on C_f, Sh_x, Nu_x, Nn_x are investigated through the use of graphs. The comparative results are presented in Table 1, together with comparisons to the findings provided by Khan et al. [32] and Ibrahim [33]. An extremely high degree of consensus was reached as a result of these outcomes. The research gap analysis table is included below in Table 2. Khan and Ibrahim analyze some parameters, In my paper, I analyze several parameters given

in Research Gap Analyzed Table 2 below. In the table, I am comparing the existing results to our results to get a good result.

Table 1. Comparision of $-f''(0)$ at various values of M and all other parameters are set to zero

M	Present study	Khan et al.	Ibrahim
0.0	1.0000	1.0000	1.0000
0.25	1.1180	1.1180	1.1180
1.0	1.4142	1.4142	1.4142
5.0	2.4495	2.4495	2.4495
10	3.3166	3.3166	3.3166
50	7.1414	7.1414	7.1414
500	22.3830	22.3830	22.3830
1,000	31.6386	31.6386	31.6386

Table 2. Research analysis gap table

Parameters	λ	Nr	Rd	Pr	Nb	Nt	σ	n	Nc	δ	E	D_f	Sc	Sr	Bi	Ec
Khan		✓		✓	✓	✓		✓								
Ibrahim		✓		✓	✓	✓		✓								
Pr study	✓	✓	✓	✓	✓	✓	✓	✓	✓	✓	✓	✓	✓	✓	✓	✓

The velocity distribution for different M values is seen in Figure 2. We noticed a narrowing of the $f'(\eta)$ with raising values of the M. When an electrically directed fluid encounters a magnetic field that generates a drag force, this phenomenon occurs as a consequence of the famous Lorentz force. Because the dragging force slows the fluid's velocity near and far from the plate, all other forces, including the Lorentz force, diminish when the fluid comes to rest.

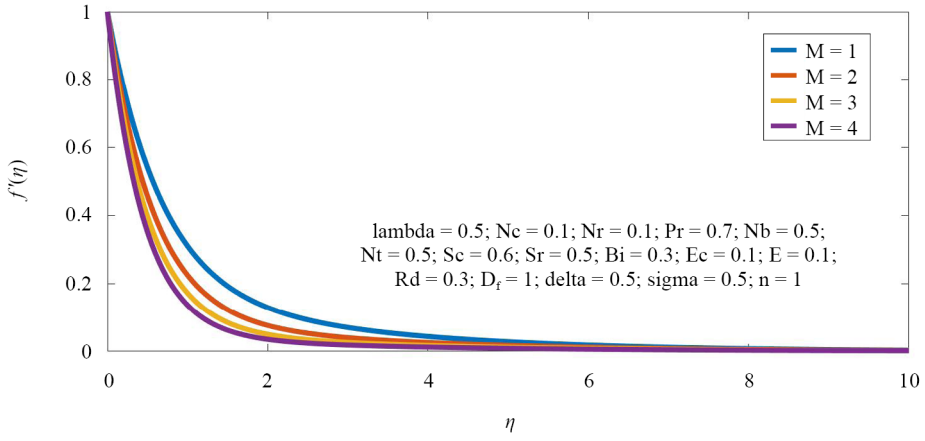

Figure 2. Magnetic parameter v/s velocity

Figure 3 displays the effect of velocity distribution, while the viscous dissipation parameter Ec is shown in Figure 4. The Ec represents the connection between the enthalpy and the kinetic energy in a flow. It stands for the internal energy conversion process that occurs when kinetic energy is exerted against the forces of a viscous fluid. A positive Eckert

number indicates that the plate is cooling or that radiation is being transferred to the liquid in the plate. Figures 3 and 4 show that the temperature and velocity are both increased due to an increase in viscous dissipative heat.

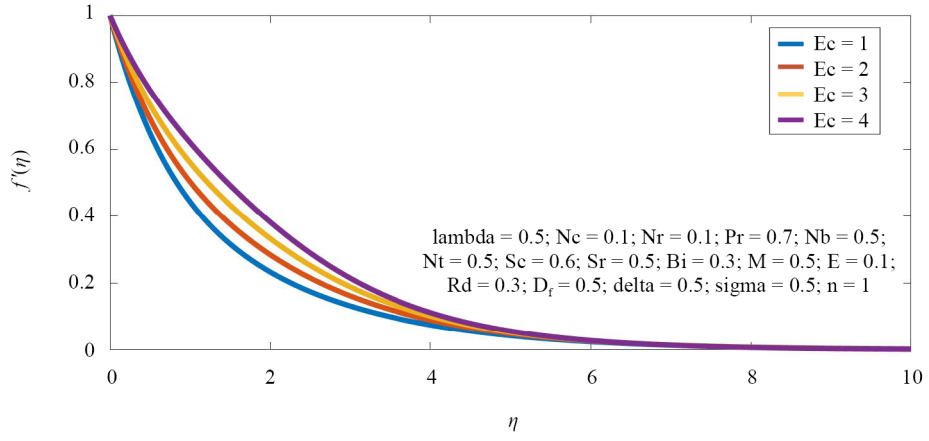

Figure 3. Eckert number v/s velocity

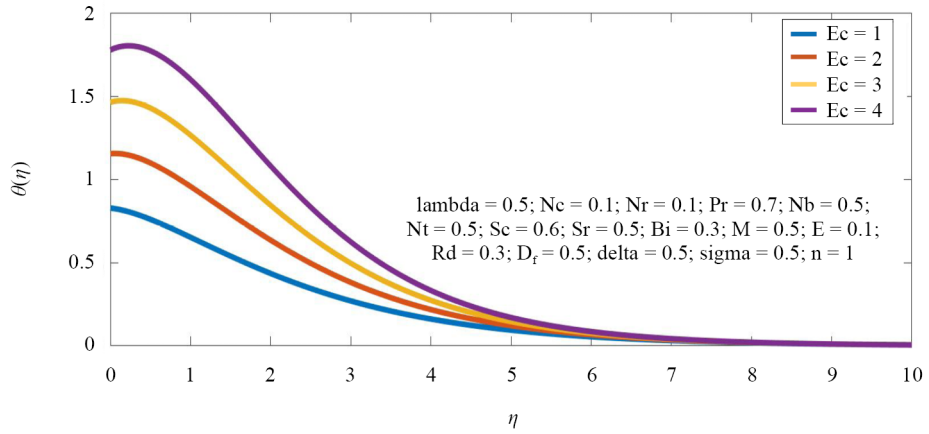

Figure 4. Eckert number v/s temperature

Figures 5-7 show the effects of the Sr on $f'(\eta)$, $\theta(\eta)$, $\chi(\eta)$ respectively. Velocity raises in relation to the soret number (Sr) is shown in Figure 5. Figure 6 displays the elevated fluid temperature as a function of the Soret number (Sr). A higher Soret number results in a faster gradient and a larger temperature variance. A stronger Soret effect causes the fluid velocity to increase. As demonstrated in Figure 7, the $\chi(\eta)$ of the fluid was further increased by the Sr. Therefore, it follows that the Dufour and Soret effects are more enthusiastically used to study mixed convection problems. The effects of Soret and Dufour on the slip parameters, chemical processes, and radiation in porous media appear to be substantial.

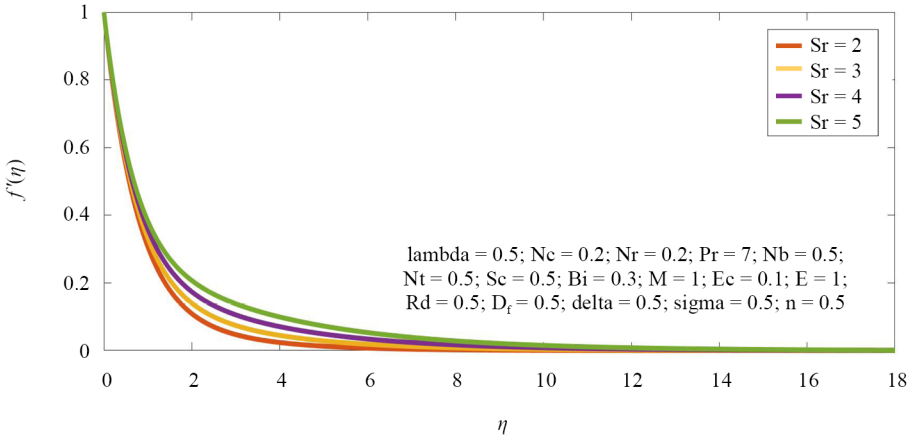

Figure 5. Soret effect v/s velocity

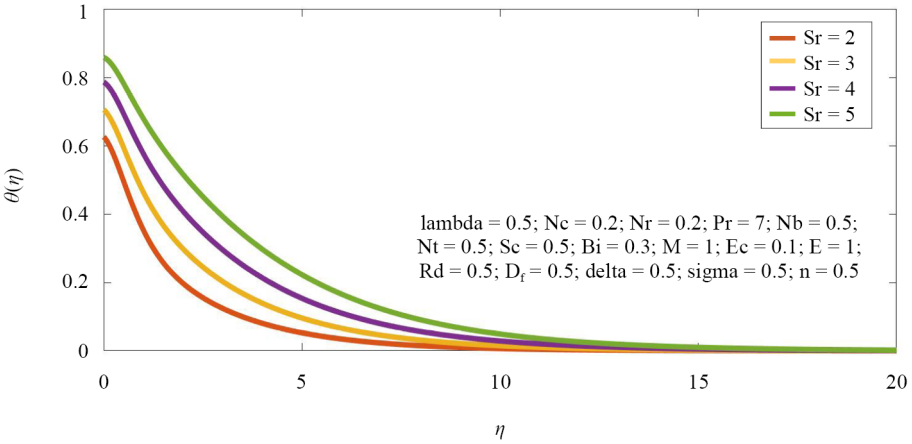

Figure 6. Soret effect v/s temperature

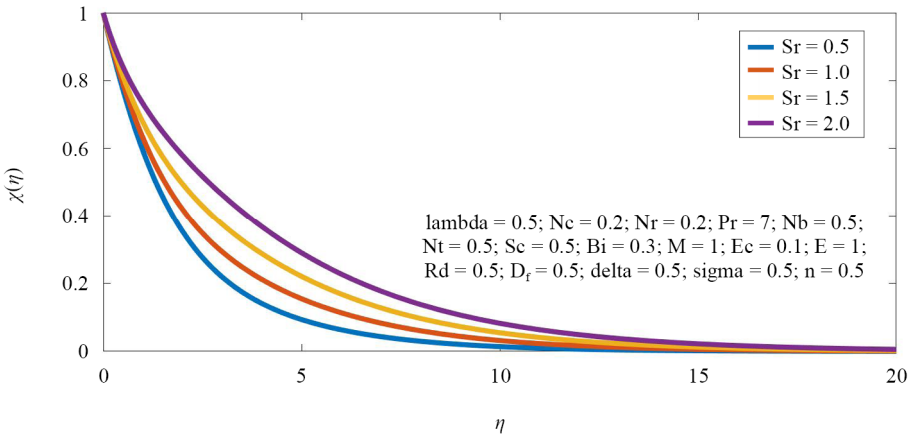

Figure 7. Soret effect v/s solute concentration

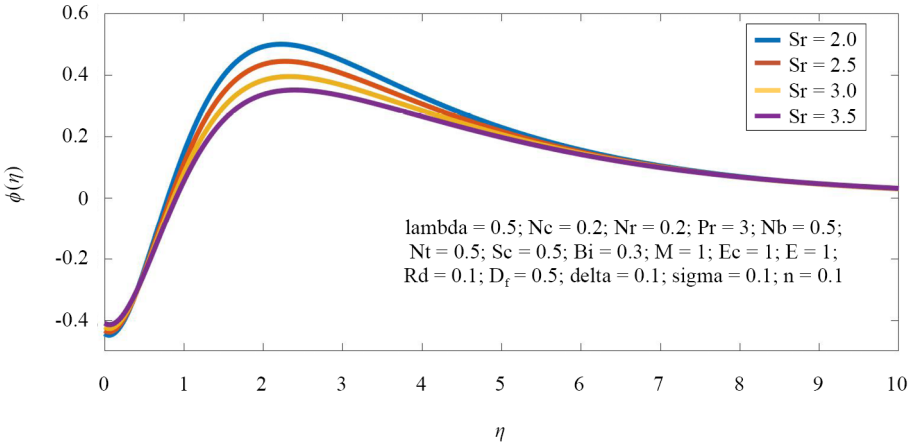

Figure 8. Soret effect v/s nanoparticle volume fraction

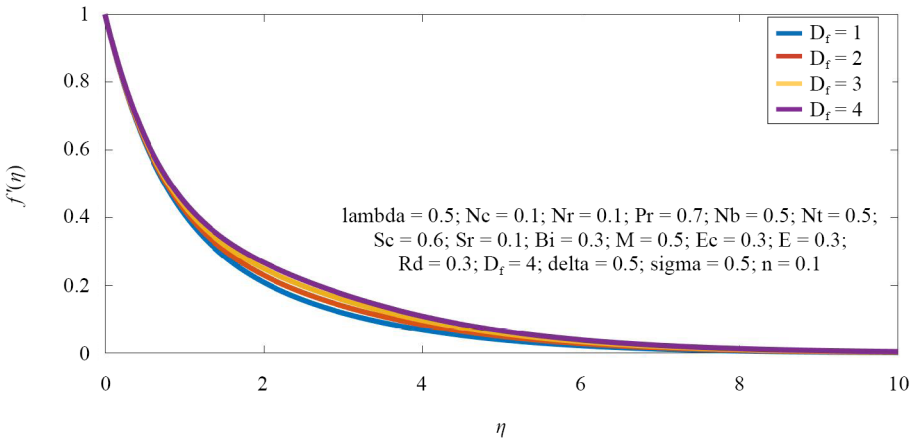

Figure 9. Dufor effect v/s velocity

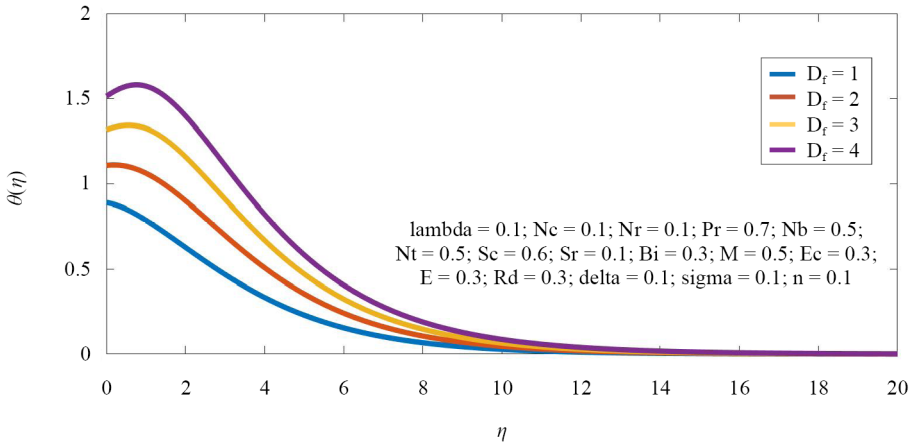

Figure 10. Dufor effect v/s temperature

As seen in Figure 8, the concentration profile is affected by the Soret number (Sr). The temperature differential, when divided by the symbol for concentration quotient, is Sr. A larger Soret number results in a larger temperature gradient. The rate of molecular diffusion is thought to be on the rise. Therefore, the rate of mass transfer increases with increasing Sr concentrations. As a result, $\phi(\eta)$ decreases.

The velocity and temperature trajectories are shown in Figures 9 and 10, respectively. (Du) denotes the proportion of the thermal energy discharge of the flow that is attributable to concentration gradients. As the Dufour number rises, the boundary layer's velocity and temperature are observed to rise as well. There is a slow but steady shift in temperature from the plate to the free stream value. Having said that, the profile abruptly collapses to zero at the BL's edge following a noticeable $f'(\eta)$ overrun near the plate. See Figure 11 for a temperature curve for different biot numbers. Both θ and the thickness of the BL are impacted by the Bi.

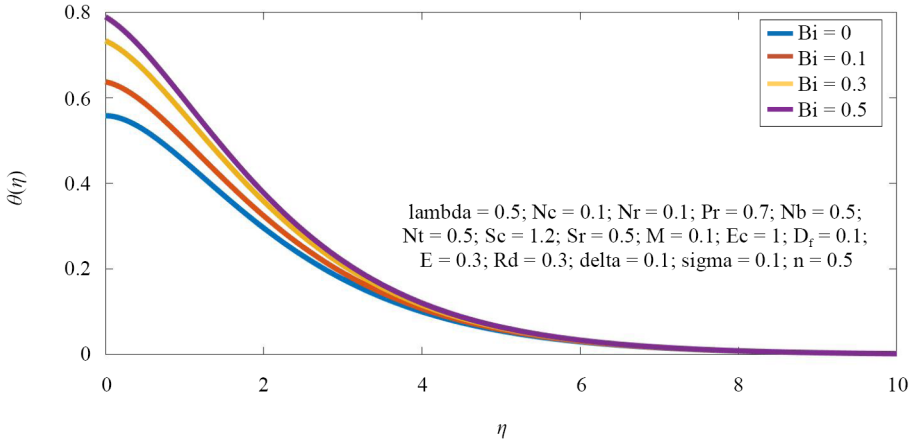

Figure 11. Biot number v/s temperature

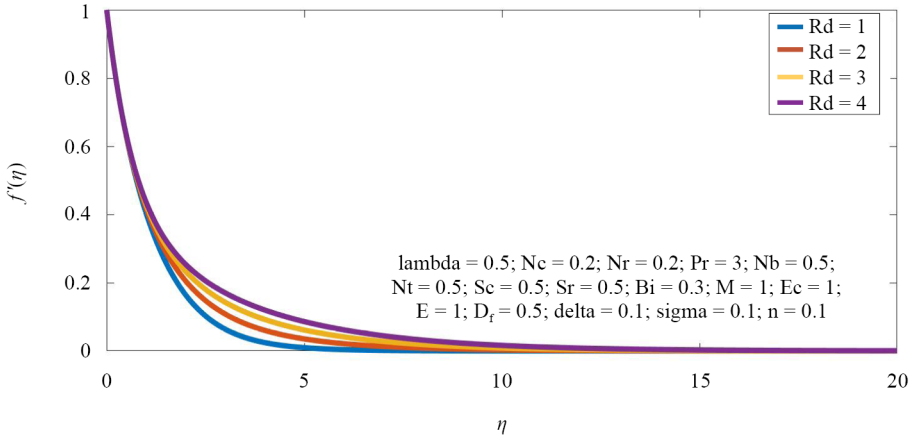

Figure 12. Thermal radiation v/s velocity

An image is made to depict the behavior of the radiation parameter Rd in Figures 12-14. Figure 12: when RD is introduced to the temperature field, it enhances the random mobility of nanoparticles. Consequently, more heat is generated due to the continuous impact. In turn, this leads to a rise. Figure 13 shows that the temperature profile and the thickness of its boundary layer are improved with larger values of the radiation parameter Rd. From a physical standpoint,

the governing fluid's boundary layer thickness and temperature profile increase when the radiation parameter Rd increases because it gives off more heat. Figure 14 shows that, in the absence of nanofluid, the nanofluid temperature and the thermal thickness of the boundary layer are maximally enhanced by the influence of thermal radiation. The nanofluid is heated to a significant degree for high values of the radiation parameter, leading to an improved temperature profile and a thicker thermal boundary layer.

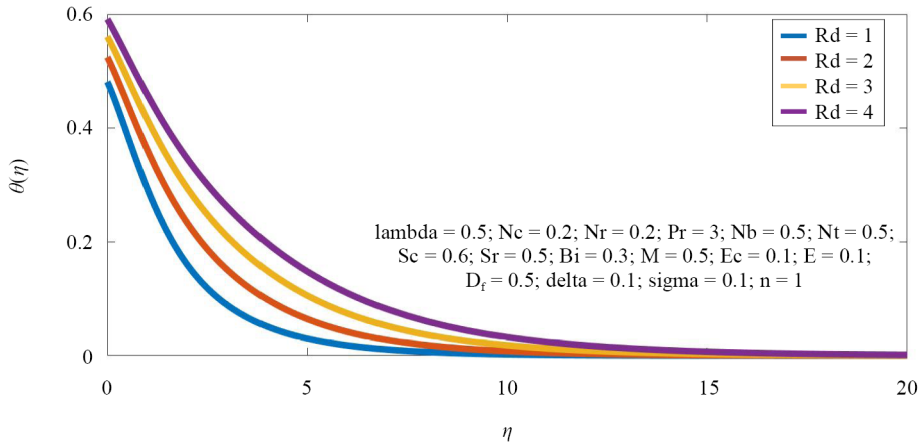

Figure 13. Thermal radiation v/s temperature

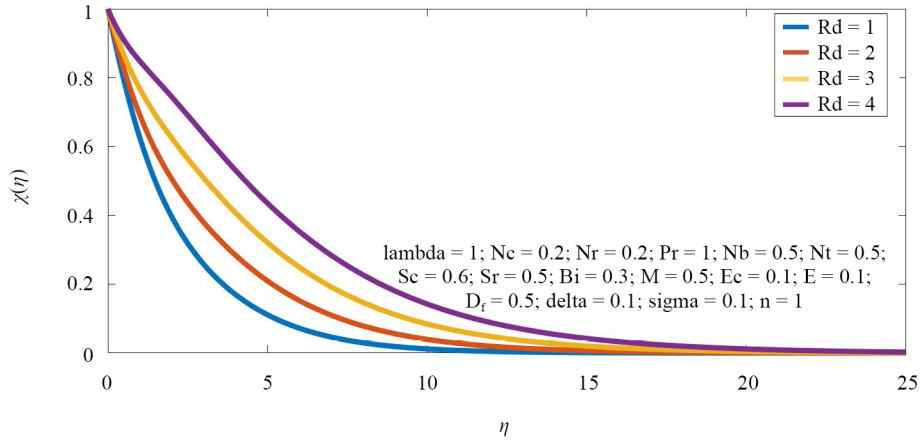

Figure 14. Thermal radiation v/s solute concentration

The effect of Sc and $-\theta'(0)$ on heat radiation is illustrated in Figure 15. Local Nusselt numbers at the local level improve radiation and Schmidt numbers. Radiation enhances heat transport, in other words. At this location, the boundary layer's breadth remains constant. In Figure 16, we can see that the skin friction and the values of the Sc and the Nt all increase as the parameter is varied. In the presence of suspended mixes of particles and fluids, which causes the nanoparticles to be displaced toward the cold region. This is because the movement of molecules of fluid in the area that is hot and the high energy levels in this region induce this displacement. Rising values of Nb in the BL region result in an increase in the rates of heat and mass transfer over the boundary layer. As shown in Figure 17, the skin friction increases as Nb is increased. The Nb is associated with a discrepancy between the BL flow and the nanoparticle concentration in a

fluid. Because the energy of fluid nanoparticles grows in relation to their mass, the skin friction of these particles rises as the Brownian motion parameter varies.

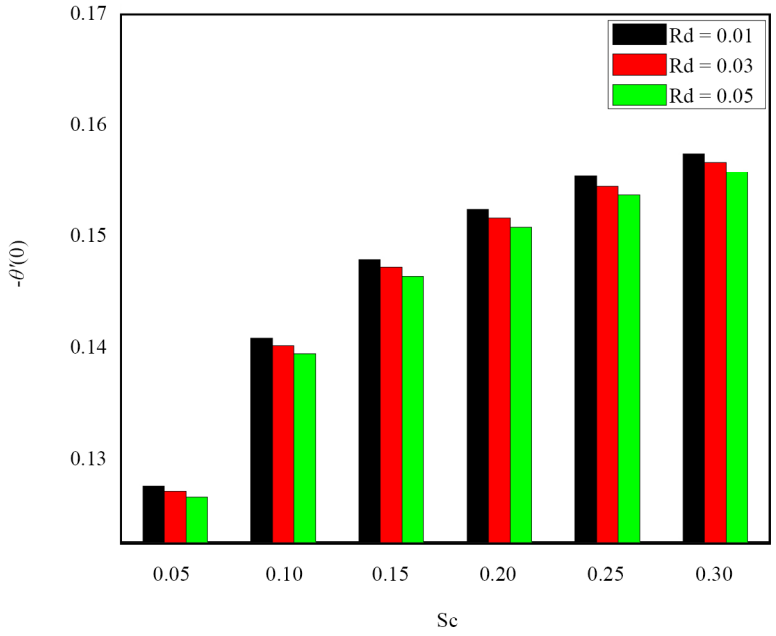

Figure 15. Nu_x v/s Rd and Sc

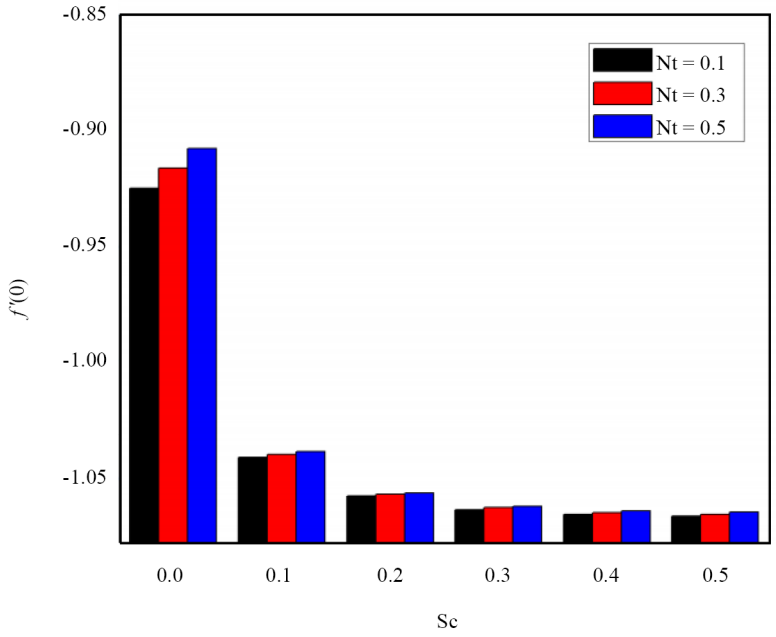

Figure 16. C_f v/s Nt and Sc

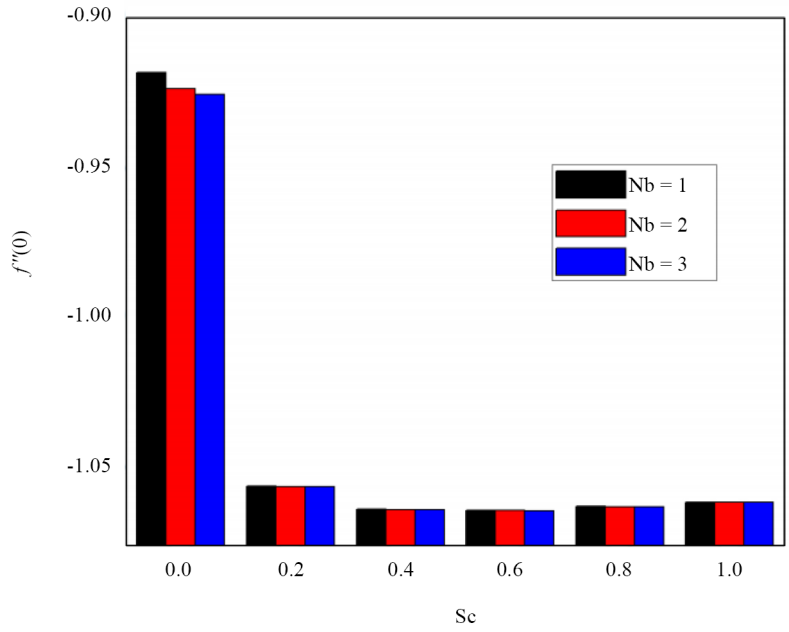

Figure 17. C_f v/s Nb and Sc

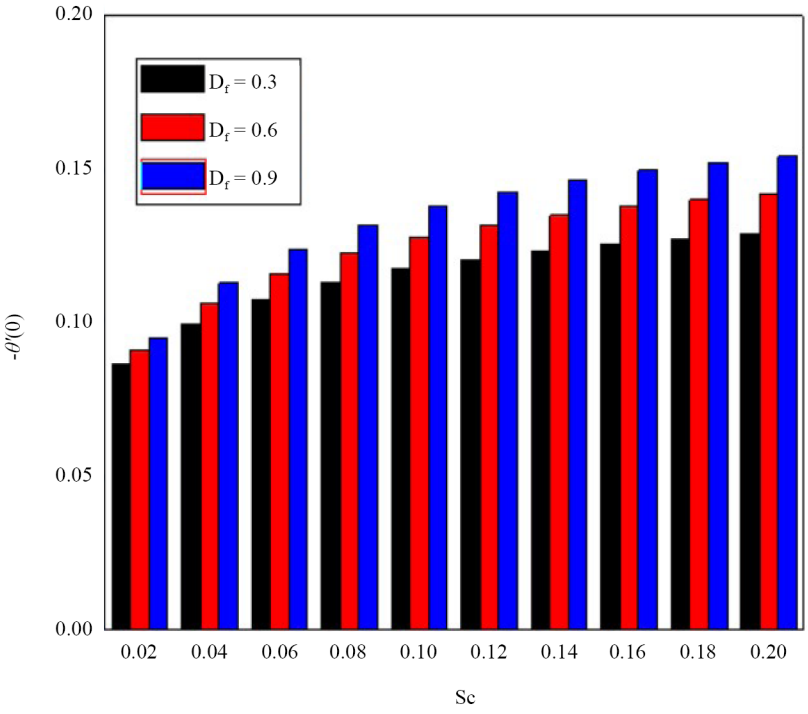

Figure 18. Nu_x v/s D_f and Sc

Figure 18 displays the different Dufour and Schmidt numbers for the local Nusselt numbers. As the nusselt number increases, a thicker boundary layer is observed when the Schmidt and Dufour effects grow. When two distinct and non-reactive fluids are allowed to mix at the same temperature, a heat flux is generated inside the system. Figure 19 displays the Sc and Ec of skin friction. In this case, the Eckert number is the joule heating parameter; there is a direct correlation

between the two variables (viscosity and thickness of the fluid), and raising the Eckert number causes viscosity to rise. C_f increases because of the growing Schmidt and Eckert numbers.

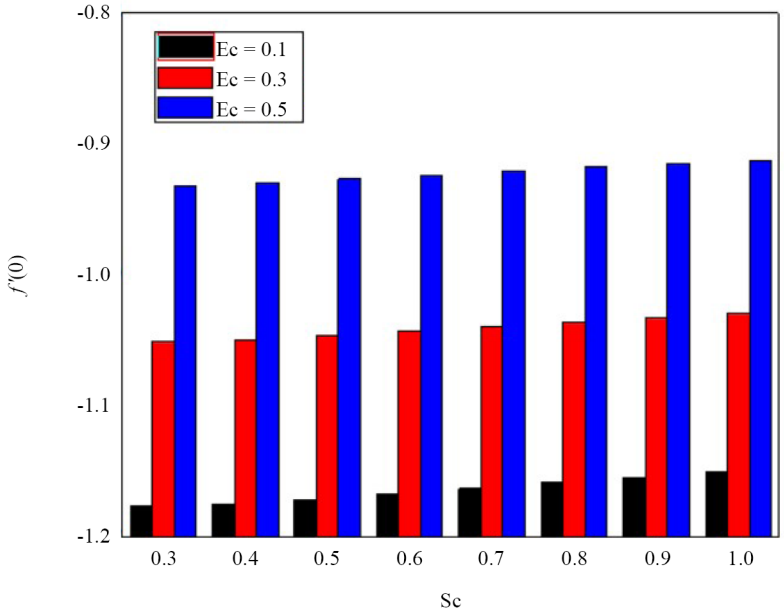

Figure 19. C_f v/s SC and Ec

6. Conclusion

In this work, numerical studies are conducted on the effects of activation energy, Soret, Dufour, and thermal radiation on the flow of MHD chemically reacting nanofluids across a vertical surface. Our investigation led us to these findings:

- Growing skin friction leads to an increase in the Eckert and Schmidt values of the Joule heating parameter.
- The local Sherwood number enhances the Schmidt and Dufour numbers.
- Increasing both the Nusselt number and the radiation with the Schmidt number.
- Increases velocity and temperature profiles by enhancing the radiation impact.
- The temperature and fluid velocity both increased as Eckert's number increased.
- The magnetic parameter increases as the fluid velocity increases.
- Dufour number increases as temperature and velocity profile increase gradually.
- A rise in the $f'(\eta)$, concentration, and $\theta(\eta)$ profile leads to a rise in the Soret number.

Conflict of interest

The authors declare no competing interest.

References

[1] Lakshmi Devi G, Niranjan H. The novelty of thermo-diffusion and diffusion-thermo, slip, temperature and concentration boundary conditions on magneto-chemically reactive fluid flow past a vertical plate with radiation. *Symmetry*. 2022; 14(8): 1496.

[2] Khan SU, Waqas H, Shehzad SA, Imran M. Theoretical analysis of tangent hyperbolic nanoparticles with combined electrical MHD, activation energy and Wu's slip features: a mathematical model. *Physica Scripta*. 2019; 94(12): 125211.

[3] Kumar KG, Rudraswamy NG, Gireesha BJ, Krishnamurthy MR. Influence of nonlinear thermal radiation and viscous dissipation on three-dimensional flow of Jeffrey nano fluid over a stretching sheet in the presence of Joule heating. *Nonlinear Engineering*. 2017; 6(3): 207-219.

[4] Khan SA, Hayat T, Alsaedi A. Irreversibility analysis in Darcy-Forchheimer flow of viscous fluid with Dufour and Soret effects via finite difference method. *Case Studies in Thermal Engineering*. 2021; 26: 101065.

[5] Shahzad F, Sagheer M, Hussain S. Numerical simulation of magnetohydrodynamic Jeffrey nanofluid flow and heat transfer over a stretching sheet considering Joule heating and viscous dissipation. *AIP Advances*. 2018; 8(6): 065316.

[6] Siddique I, Nadeem M, Awrejcewicz J, Pawłowski W. Soret and Dufour effects on unsteady MHD second-grade nanofluid flow across an exponentially stretching surface. *Scientific Reports*. 2022; 12(1): 1-4.

[7] Pal D, Das B, Vajravelu K. Magneto-Soret-Dufour thermo-radiative double-diffusive convection heat and mass transfer of a micropolar fluid in a porous medium with Ohmic dissipation and variable thermal conductivity. *Propulsion and Power Research*. 2022; 11(1): 154-170.

[8] Ali L, Ali B, Habib D, Al Mdallal Q. Finite element analysis on the thermo-convective non-isothermal nanofluid flow in MHD Hall generator system with Soret and Dufour effects. *Case Studies in Thermal Engineering*. 2022; 39: 102389.

[9] Muhammad T, Hayat T, Shehzad SA, Alsaedi A. Viscous dissipation and Joule heating effects in MHD 3D flow with heat and mass fluxes. *Results in Physics*. 2018; 8: 365-371.

[10] Mahanthesh B, Gireesha BJ. Scrutinization of thermal radiation, viscous dissipation and Joule heating effects on Marangoni convective two-phase flow of Casson fluid with fluid-particle suspension. *Results in Physics*. 2018; 8: 869-878.

[11] Niranjan H, Sivasankaran S, Bhuvaneswari M. Chemical reaction, Soret and Dufour effects on MHD mixed convection stagnation point flow with radiation and slip condition. *Scientia Iranica*. 2017; 24(2): 698-706.

[12] Ullah Z, Bilal M, Sarris IE, Hussanan A. MHD and thermal slip effects on viscous fluid over symmetrically vertical heated plate in porous medium: keller box analysis. *Symmetry*. 2022; 14(11): 2421.

[13] Sreedevi G, Prasada Rao DRV, Makinde OD, Ramana Reddy GV. Soret and Dufour effects on MHD flow with heat and mass transfer past a permeable stretching sheet in presence of thermal radiation. *Indian Journal of Pure and Applied Physics (IJPAP)*. 2017; 55(8): 551-563.

[14] Ali U, Irfan M, Akbar NS, Ur Rehman K, Shatanawi W. Dynamics of Soret-Dufour effects and thermal aspects of Joule heating in multiple slips Casson-Williamson nanofluid. *International Journal of Modern Physics B*. 2024; 38(16): 2450206.

[15] Ahammad NA, Krishna MV. Numerical investigation of chemical reaction, Soret and Dufour impacts on MHD free convective gyrating flow through a vertical porous channel. *Case Studies in Thermal Engineering*. 2021; 28: 101571.

[16] Mondal H, Pal D, Chatterjee S, Sibanda P. Thermophoresis and Soret-Dufour on MHD mixed convection mass transfer over an inclined plate with non-uniform heat source/sink and chemical reaction. *Ain Shams Engineering Journal*. 2018; 9(4): 2111-2121.

[17] Shankar Goud B, Dharmendar Reddy Y, Mishra S. Joule heating and thermal radiation impact on MHD boundary layer Nanofluid flow along an exponentially stretching surface with thermal stratified medium. *Proceedings of the Institution of Mechanical Engineers, Part N: Journal of Nanomaterials, Nanoengineering and Nanosystems*. 2023; 237(3-4): 107-119.

[18] Naseem T, Fatima U, Munir M, Shahzad A, Kausar N, Nisar KS, et al. Joule heating and viscous dissipation effects in hydromagnetized boundary layer flow with variable temperature. *Case Studies in Thermal Engineering*. 2022; 35: 102083.

[19] Mat Noor NA, Shafie S, Hamed YS, Admon MA. Soret and Dufour effects on MHD squeezing flow of Jeffrey fluid in horizontal channel with thermal radiation. *Plos One*. 2022; 17(5): e0266494.

[20] Padmaja K, Rushi Kumar B. Viscous dissipation and chemical reaction effects on MHD nanofluid flow over a vertical plate in a rotating system. *ZAMM-Journal of Applied Mathematics and Mechanics/Zeitschrift für Angewandte Mathematik und Mechanik*. 2023; 103(9): e202200471.

[21] Ghachem K, Kolsi L, Khan SU, Abbas T, Maatki C, Saeed M. Soret and Dufour aspect of viscoelastic fluid due to moving cylinder with viscous dissipation and convective boundary conditions. *Journal of the Indian Chemical Society*. 2023; 100(2): 100913.

[22] Kumar BR. Viscous dissipation and chemical reaction effects on mhd nanofluid flow over a vertical plate in a rotating system. *SSRN Journal*. 2022; 2022: 1-15.

[23] Ashraf M, Ilyas A, Ullah Z, Ali A. Combined effects of viscous dissipation and magnetohydrodynamic on periodic heat transfer along a cone embedded in porous medium. *Proceedings of the Institution of Mechanical Engineers, Part E: Journal of Process Mechanical Engineering*. 2022; 236(6): 2325-2335.

[24] Mahanthesh B, Gireesha BJ, Gorla RSR. Unsteady three-dimensional MHD flow of a nano Eyring Powell fluid past a convectively heated stretching sheet in the presence of thermal radiation, viscous dissipation and Joule heating. *Journal of the Association of Arab Universities for Basic and Applied Sciences*. 2017; 23: 75-84.

[25] Muduly MM, Rath PK, Karc P, Swain K. Effects of Joule heating and viscous dissipation on Casson nanofluid flow over a stretched sheet with chemical reaction. *Journal of Computational Applied Mechanics*. 2022; 54(4): 478-493.

[26] Huang JS. Chemical reaction and activation energy on heat and mass transfer for convective flow along an inclined surface in Darcy porous medium with Soret and Dufour effects. *Journal of Mechanics*. 2023; 39: 88-104.

[27] Seid E, Haile E, Walelign T. Multiple slip, Soret and Dufour effects in fluid flow near a vertical stretching sheet in the presence of magnetic nanoparticles. *International Journal of Thermofluids*. 2022; 13: 100136.

[28] Devi GL, Hari N. Influence of Soret and Dufour, activation energy on MHD chemically reacting nanofluid flow past a vertical surface with radiation. *Latin American Applied Research*. 2022; 52: 239-246.

[29] Kumar RK, Kumar GV, Raju CSK, Shehzad SA, Varma SVK. Analysis of Arrhenius activation energy in magnetohydrodynamic Carreau fluid flow through improved theory of heat diffusion and binary chemical reaction. *Journal of Physics Communications*. 2018; 2(3): 035004.

[30] Sivasankaran S, Niranjan H, Bhuvaneswari M. Chemical reaction, radiation and slip effects on MHD mixed convection stagnation-point flow in a porous medium with convective boundary condition. *International Journal of Numerical Methods for Heat and Fluid Flow*. 2017; 27(2): 454-470.

[31] Yesodha P, Bhuvaneswari M, Sivasankaran S, Saravanan K. Convective heat and mass transfer of chemically reacting fluids with activation energy along with Soret and Dufour effects. *Materials Today: Proceedings*. 2021; 42: 600-606.

[32] Yesodha P, Bhuvaneswari B, Sivasankaran S, Saravanan K. Convective heat and mass transfer of chemically reacting fluids with activation energy with radiation and heat generation. *Journal of Thermal Engineering*. 2021; 7(5): 1130-1138.

[33] Ibrahim W. Magnetohydrodynamics (MHD) flow of a tangent hyperbolic fluid with nanoparticles past a stretching sheet with second order slip and convective boundary condition. *Results in Physics*. 2017; 7: 3723-3731.

[34] Ullah Z, Ashraf M, Zia S, Ali I. Surface temperature and free-stream velocity oscillation effects on mixed convention slip flow from surface of a horizontal circular cylinder. *Thermal Science*. 2020; 24(Suppl 1): 13-23.

[35] Gaffar SA, Prasad VR, Bég OA. Numerical study of flow and heat transfer of non-Newtonian tangent hyperbolic fluid from a sphere with Biot number effects. *Alexandria Engineering Journal*. 2015; 54(4): 829-841.

[36] Makinde OD, Aziz A. Boundary layer flow of a nanofluid past a stretching sheet with a convective boundary condition. *International Journal of Thermal Sciences*. 2011; 50(7): 1326-1332.

[37] Rahman MM, Eltayeb IA. Radiative heat transfer in a hydromagnetic nanofluid past a non-linear stretching surface with convective boundary condition. *Meccanica*. 2013; 48: 601-615.

[38] Swain BK, Parida BC, Kar S, Senapati N. Viscous dissipation and joule heating effect on MHD flow and heat transfer past a stretching sheet embedded in a porous medium. *Heliyon*. 2020; 6(10): e05338.